8th International Congress of Information and Communication Technology, ICICT 2019

Boundary Influence on MCG Sparse Inverse Problem

Lu Bing[a],*, Xiaolei Han[a], Wen Si[a], Fuqiang Liu[a], Jiang Yu[a], Rong Tan[a]

aSchool of Information and Computer Science, Shanghai Business School, 123 Feng Pu Avenue, Shanghai 201400, P.R. China

Abstract

In this paper, we discuss the influence for MCG (magnetocardiography) sparse inverse problem when conductivity uncertainty exists, through a heart- torso model by boundary element method. Fixed and moving current dipoles are designed in order to study the influence of cardiac conductivity on source reconstruction. Two indicators including the position error and the reconstructed source mean distance are used to evaluate the results. The simulating results demonstrate that the index of dipole source reconstruction outside the heart is better than that inside the heart, that is, the complicated conductivity has a greater impact on source reconstruction. In addition, the position error of the source by modified FOCUSS reconstruction is close to that of the fast greedy sparse method, and sometimes better than the latter.

Keywords: MCG; Sparse inverse problem; Heart-torso model; Conductivity

1. Introduction

In recent years, research on the heart-torso model has continued to deepen. In 1987, Jukka Sarvas derived basic equations for the biomagnetic positive and inverse problems [1]. In 1996, P Czapski studied the effects of conductivity media on the magnetic field of the heart under a real heart-torso model[2]. In 1998, G. Fischer et al. demonstrated the effectiveness of applying BEM (boundary element method) to ECG (electrocardiogram) positive and inverse problems [3]. In 2007, M.Stenroos et al. presented a Matlab software package where they used BEM to

* Corresponding author.
    E-mail address: betty20006@163.com

10.1016/j.procs.2019.06.034

solve quasi-static volume conductors [4]. Keller et al. studied the effect of dielectric conductivity on positive ECG problems [5]. In the same year, Mostafa Bendahmane et al. studied the excitatory propagation of the heart in isotropic media by the finite volume conductor method [6]. In 2013, Hüsnü Dal et al. proposed a FEM method for the bidomain model of cardiac electromagnetic mechanisms [7]. Xia Lin et al. of Zhejiang University in China also conducted research on constructing a precise heart-torso model [8,9].

This paper investigates the effects of conductivity uncertainty on cardiac magnetic reconstruction through a simple heart-torso model constructed with BEM. The goal is to analyze the extent to which cardiac conductance affects the magnetic field. Commonly used numerical calculation methods are: Finite element method (FEM) [10], Finite difference method (FDM) [11], Boundary element method (BEM) [12], and Finite volume method (FVM) [13].

2. Magnetic field in inhomogeneous medium

Let G be a bounded biological conductor with different internal conductivity and zero internal conductivity. The different conductivity boundary surfaces are set to S_j, $j = 1, \cdots, K$. Then the integral equation corresponding to the magnetic field can be obtained as [1]:

$$\boldsymbol{B(r)} = \frac{\mu_0}{4\pi} \int_G \boldsymbol{J}^i(\boldsymbol{r'}) \times \frac{\boldsymbol{r-r'}}{|\boldsymbol{r-r'}|^3} dv' - \frac{\mu_0}{4\pi} \sum_{j=1}^K (\sigma_j' - \sigma_j'') \int_{S_j} \boldsymbol{V(r')(r')} \times \frac{\boldsymbol{r-r'}}{|\boldsymbol{r-r'}|^3} dS_j = \boldsymbol{B_0(r)} + \boldsymbol{B_{Vol}(r)} \quad (1)$$

Where, $\boldsymbol{B}$ is the magnetic field at the detection point, $\boldsymbol{r}$ is the position of the measurement point, $\boldsymbol{V}$ is the voltage on the boundary surface, $\boldsymbol{J}^i$ is the internal current density of G, and σ_j' and σ_j'' are the internal and external conductivity of S_j, respectively. $\boldsymbol{B_0}$ is the magnetic field generated by $\boldsymbol{J}^i$ in a uniform space, $\boldsymbol{B_{Vol}}$ is the magnetic field generated by the volume current, and μ_0 is the vacuum permeability. The integral equation for the boundary voltage $\boldsymbol{V}$ [1, 4]:

$$\boldsymbol{V(r)} = \frac{2\sigma_s}{\sigma_k' + \sigma_k''} \boldsymbol{V_0(r)} - \sum_{j=1}^K \frac{\sigma_j' - \sigma_j''}{2\pi(\sigma_k' + \sigma_k'')} \int_{S_j} \boldsymbol{V(r')n(r')} \cdot \frac{\boldsymbol{r-r'}}{|\boldsymbol{r-r'}|^3} dS_j \quad (2)$$

Where, σ_s is the conductivity of the area contained in $\boldsymbol{J}^i$, and $\boldsymbol{n}$ is the unit normal vector of the point on the boundary surface, in addition,

$$\boldsymbol{V_0(r)} = \frac{1}{4\pi\sigma_s} \int_G \boldsymbol{J}^i(\boldsymbol{r}) \cdot \frac{\boldsymbol{r-r'}}{|\boldsymbol{r-r'}|^3} dv' \quad (3)$$

Indicates the voltage generated by $\boldsymbol{J}^i$ in a uniform medium.

In practical applications, the above integral equation needs to be discretized. Suppose the number of measuring points is M, the number of current dipoles is Q, and the number of triangular boundary elements is P. Equation (1) can be approximated as [1,4]:

$$\boldsymbol{B} = \boldsymbol{B_0} + \boldsymbol{B_{Vol}} = \boldsymbol{A_{J \to B} J} + \boldsymbol{A_{V \to B} V} \quad (4)$$

Where, the magnetic fields $\boldsymbol{B}$, $\boldsymbol{B_0}$ and $\boldsymbol{B_{Vol}}$ are $M \times 1$ vectors, $\boldsymbol{J}$ is a dipole moment, and is a $N = 3Q \times 1$ vector, that is, each dipole has three orthogonal components, $\boldsymbol{J} = [\boldsymbol{J_x}, \boldsymbol{J_y}, \boldsymbol{J_z}]$. The potential $\boldsymbol{V}$ is a $P \times 1$ vector, $\boldsymbol{A_{J \to B}}$ is a $M \times N$ matrix, and $\boldsymbol{A_{V \to B}}$ is a $M \times P$ matrix. Equation (2) can be expressed as [1] using the weighted residual method equation:

$$V = A_V V_0 = A_V A_{J \to V} J \tag{5}$$

Where, A_V is a $P \times P$ matrix and $A_{J \to V}$ is a P×N matrix. Substituting equation (5) into (4) gives:

$$B = (A_{J \to B} + A_{V \to B} A_V A_{J \to V}) J = LJ \tag{6}$$

Where, $L = A_{J \to B} + A_{V \to B} A_V A_{J \to V}$ is the lead-field matrix, which reflects the dielectric properties of the conducting medium [1]. $A_{J \to B}$ is the lead matrix under the infinite uniform medium model. According to the boundary element method, the relationship between the current density inside the conductor and the magnetic field can be approximated by a linear equation. Similar to the lead matrix in the infinite uniform medium model, when B is a known quantity in equation (6) and J is an unknown quantity, the equations contain M equations with $N = 3Q$ unknowns, where $N \ll 3M$. Therefore, the system of equations is underdetermined.

3. Heart-Torso Model

In order to study the influence of heart boundary on source reconstruction, this paper uses a heart-torso model based on the above boundary element method [14]. This model consists of the trunk, heart and two lungs. The three parameters of the torso in the geometry parameter represent the height of the cylinder, the major and minor axes of the ellipse, along with three dimensions of the three ellipsoids of the heart and the left and right lungs.

In 2010, Keller et al.'s study of cardiac conductivity showed that the ratio of the maximum to the minimum of the conductivity of the trunk, heart, and lung was 1.1, 9.0, and 3.4, respectively [5]. The conductivity of the trunk and lungs with smaller ratios were set to fixed values of 0.216 S/m and 0.389 S/m, respectively. In order to investigate the influence of conductivity, a cardiac-torso model with different conductivity is used. The torso conductivity ratios are 0.237, 0.513, 0.665, 0.846, 1.064, 1.299, 1.599, 1.799, 1.998, and 2.322, respectively. Their corresponding models are M_1-M_8, and the infinite uniform medium model is M_0.

4. Influence of Conductivity Uncertainty on Source Reconstruction

In order to study the influence of cardiac conductivity on source reconstruction, we use a single current dipole as a simulation source to generate a simulated magnetic field through the setting of conductivity, and solve the inverse problem by setting different conductivity. According to the conductivity of M_0-M_8, the lead-field matrix L_0-L_8 can be obtained by the boundary element method.

4.1. Evaluation index

In this section, two indicators including the position error (PE) and the reconstructed source mean distance (MD) are used to evaluate the results of the source reconstruction [14]. The position error indicates the accuracy of the positioning, and the average distance of the reconstructed source indicates the concentration of the energy of the reconstructed source. The smaller the position error is, the more accurate the position of the reconstruction source is. The smaller the average distance of the reconstruction source is, the more concentrated the energy of the reconstruction source is. The calculation formula for the two indicators is as follows:

$$\mathrm{PE} = |L_d - L_{rs}| \tag{7}$$
$$\mathrm{MD} = \frac{1}{N} \sum_{i=1}^{N} (L_i - L_{rsm}) \tag{8}$$

Where, L_d is the position of a given dipole and L_{rs} is the location of the reconstruction source. The source of L_i is expressed as follows: It is assumed that the maximum strength of the reconstructed source is S_{max}, and the number

of points larger than$(1 - \frac{1}{e})S_{max}$ has a total of N points, and L_i is the i-th point. The average distance from these points to the location of the maximum intensity point of the reconstruction source, L_{rsm}, is defined as MD.

4.2. Simulation results of fixed current dipole source reconstruction

In the simulation, it is assumed that the source is located in a plane with vertices of (4, 4, 10) and (20, 20, 8). The minimum spacing of the grid is 0.1cm. Dipoles 1 and 7 are outside the heart, dipoles 2 and 6 are close to the heart, and dipoles 3-5 are inside the heart. The variation law of dipoles is divided into two cases. Case 1: Direction of the dipole moment is fixed and the intensity is sinusoidal; Case 2: Direction and intensity of dipole moment changes randomly. To discuss the effect of noise on source reconstruction, we add a Gaussian white noise with a signal-to-noise ratio of 25 dB to the generated magnetic field.

Fig. 1 shows the average position error of the source reconstruction at seven different locations. The magnetic field reconstructed from the source is generated in M_1. It can be seen that when the conductivity of the generated magnetic field is consistent with the source reconstruction (that is, when the forward problem and the inverse problem model are used), the position error is zero, and the reconstructed source radius is also concentrated to a point. When the conductivity error increases, the average position error also increases.
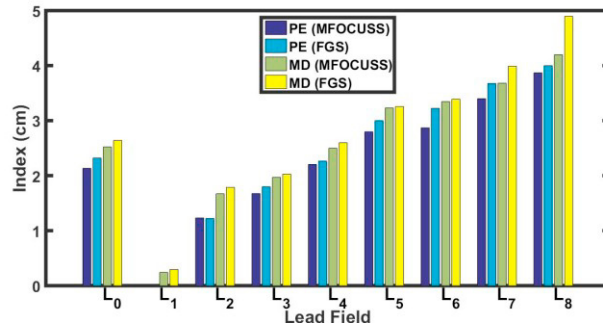
Fig. 1. Average index of reconstruction of the same depth fixed dipole source.
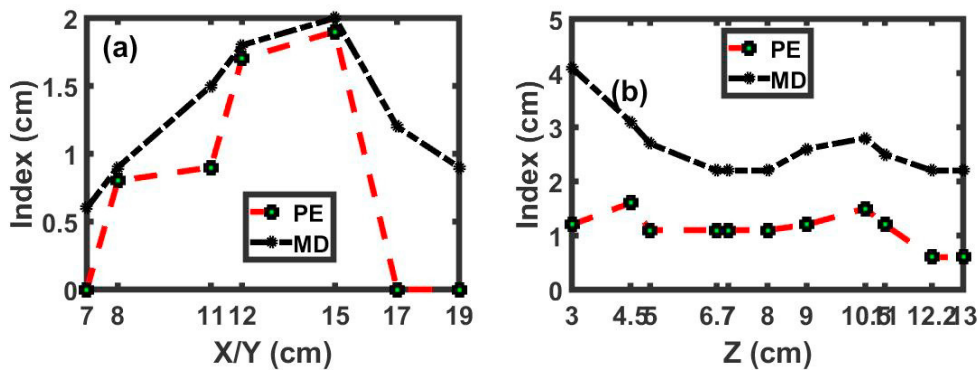
Fig. 2. Index for reconstruction of dipole sources at different locations using the L_2 lead field. (a) same depth dipole; (b) different depth dipoles.

Fig. 2 shows the index for reconstruction of dipole sources at different locations using the $\boldsymbol{L}_2$ lead field. Fig. 2 (a) shows the source reconstruction index for the same depth dipole, and Fig. 2 (b) shows the different depth result. We give the curve of MFOCUSS (Modified FOCUSS) as a reference [15]. The trend from the curve in Fig. 2(a) shows that the dipole outside the heart is separated from the measurement plane by a single conductivity boundary, and the dipole inside the heart and the measurement plane are separated by two conductivity boundaries. Therefore, the

results of the dipole source reconstruction index outside the heart are better than that inside the heart. It can be seen from Fig. 2 (b) that starting from 6cm, the index of source reconstruction increases with depth, and when it exceeds 10cm, the value of the indicator begins to decrease again. This is because the depth of 6-10cm is basically the inside of the heart, and the conductivity is relatively complicated, the influence on the source reconstruction is relatively large. The effect when the depth is less than 5cm may be caused by the proximity of the measuring point.

4.3. Simulation results of moving current dipole source reconstruction

For moving current dipoles, we use the MFOCUSS and FGS (fast greedy sparse) methods [16] for source reconstruction. The magnetic field reconstructed from the source is generated in M_1. Similar to fixed dipoles, the results of different source reconstruction methods using the same positive problem model are almost identical without considering noise. Fig. 3 shows the average value of the index reconstructed by the MFOCUSS method for moving dipoles. The activity of the position error is consistent with the source reconstruction of the fixed current dipole.
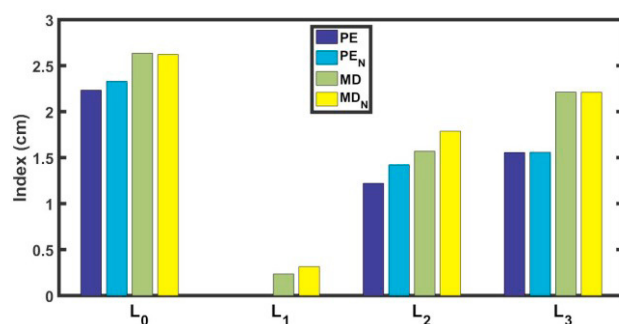
Fig. 3. Value of the index reconstructed for moving dipoles.

5. Conclusions

This paper analyzes the influence of uncertainty of conductivity on source reconstruction through simulation. A simple heart-torso model constructed by the boundary element method is used. Through the indicators of source reconstruction, we can see the effect of the positive problem model on the source reconstruction results. When the conductivity of the generated magnetic field is consistent with the conductivity of the model, the MFOCUSS and FGS methods can effectively reconstruct a given source. When the conductivity of the model is inconsistent with that of the magnetic field, the average position error may occur. The index of dipole source reconstruction outside the heart is better than the index of dipole source reconstruction inside the heart, that is, the complex conductivity has a greater impact on source reconstruction. In addition, the position error of the source of MFOCUSS reconstruction is close to that of the FGS method, and sometimes better than the latter.

Acknowledgement

References

1. Jukka S. Basic mathematical and electromagnetic concepts of the biomagnetic inverse problem. Physics in Medicine and Biology, 1987, Vol.32(1): 11~22.
2. Czapski P, Ramon C, Huntsman L L, et al. Effects of tissue conductivity cariations on the cardiac magnetic fields simulated with a realistic heart-torso model. Physics in Medicine and Biology, 1996, Vol.41(8): 1247~1263.
3. Fischer G, Tilg B, Wach P, et al. Analytical validation of the BEM-application of the BEM to the electrocardiographic forward and inverse problem. Computer Methods and Programs in Biomedicine, 1998, Vol.55(2):99~106.
4. Stenroos M, Mantynen V, Nenonen J.A Matlab library for solving quasi-static volume conduction problems using the boundary element method. Computer Methods and Programs in Biomedicine, 2007,Vol.88(3): 256~263.
5. U.J.Keller D, M.Weber F, Seemann G, et al. Ranking the influence of tissue conductivities on forward-calculated ECGs. IEEE Transactions on Biomedical Engineering, 2010, Vol.57(7): 1568~1576.
6. Mostafa B, Raimund B, Ricardo R B. A finite volume scheme for cardiac propagation in media with isotropic conductivities. Mathematics and Computers in Simulation, 2010, Vol. 80(9): 1821~1840.
7. Hüsnü D, Serdar G, Michael K,et al. A fully implicit finite element method for bidomain models of cardiac electromechanics. Computer Methods in Applied Mechanics and Engineering Volume, 2013, Vol.253(1): 323~336.
8. Xai Ling, Ye Xuesong, Huo Meimei. Simulation of body surface electrocardiogram based on dynamic heart model. Chinese Biomedical Engineering, 2006, Vol.25(3): 257~262(In Chinese).
9. Xai Ling, Ye Xuesong, Huo Meimei. 3D motion analysis of right ventricle based on electrophysiological composite heart model. Journal of biomedical engineering, 2007, Vol.24(1): 110~115(In Chinese).
10. Yang J S, Yang N. A brief review of FEM software technique. Advances in Engineering Software, 1993, Vol.17(3): 195~200.
11. Cubric D, Lencova B, Read F H, et al.Comparison of FDM, FEM and BEM for electrostatic charged particle. Nuclear Instruments and Methods in Physics Research Section A: Accelerators, Spectrometers, Detectors and Associated Equipment,1999,Vol.427(1-2): 357~362.
12. Yu K H, Kadarman A H, Djojodihardjo HA. Development and implementation of some BEM variants-A critical review. Engineering Analysis with Boundary Elements, 2010, Vol.34(10): 884~899.
13. Jiří M, Otto S, Miloslav T, et al. Modelling of processes in fractured rock using FEM/FVM on multidimensional domains. Journal of Computational and Applied Mathematics, 2008, Vol.215(2): 495~502.
14. Weiyuan Wang, etc. Distributed current source reconstruction of magnetocadiography and its accuracy analysis.2014, aps.62.148703.
15. Lu Bing, Shiqin Jiang. Magnetocardiography T wave signals reconstruction with smoothed sparse constraint. International Conference on System Simulation, 2012: 298~301.
16. Lu Bing, Weiyuan Wang, Yongliang Wang, Shiqin Jiang. MCG source reconstruction based on greedy sparse method. Acta Physica Sinica, 2013, Vol.62(11), 118703.